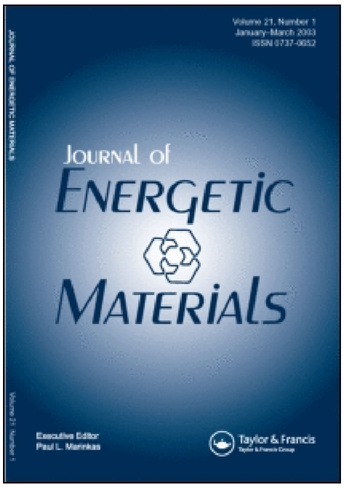

Journal of Energetic Materials
Publication details, including instructions for authors and subscription information:
http://www.informaworld.com/smpp/title~content=t713770432

Development of Particle Concentration Distributions and Burn Rate Gradients upon Shear-Induced Particle Migration during Processing of Energetic Suspensions

Melquiades Allende[a]; David F. Fair[b]; Dilhan M. Kalyon[c]; Donald Chiu[b]; Sam Moy[b]
[a] Stevens Institute of Technology, [b] U.S. Army TACOM-ARDEC, Picatinny Arsenal, NJ [c] Stevens Institute of Technology,Castle Point on Hudson, Hoboken, NJ

To cite this Article Allende, Melquiades , Fair, David F. , Kalyon, Dilhan M. , Chiu, Donald and Moy, Sam(2007) 'Development of Particle Concentration Distributions and Burn Rate Gradients upon Shear-Induced Particle Migration during Processing of Energetic Suspensions', Journal of Energetic Materials, 25: 1, 49 — 67

To link to this Article: DOI: 10.1080/07370650601107203

URL: http://dx.doi.org/10.1080/07370650601107203

Journal of Energetic Materials, 25: 49–67, 2007
Copyright © Taylor & Francis Group, LLC
ISSN: 0737-0652 print/1545-8822 online
DOI: 10.1080/07370650601107203

Development of Particle Concentration Distributions and Burn Rate Gradients upon Shear-Induced Particle Migration during Processing of Energetic Suspensions

MELQUIADES ALLENDE*
Stevens Institute of Technology

DAVID F. FAIR
U.S. Army TACOM-ARDEC, Picatinny Arsenal, NJ

DILHAN M. KALYON
Stevens Institute of Technology,
Castle Point on Hudson, Hoboken, NJ

DONALD CHIU
SAM MOY
U.S. Army TACOM-ARDEC, Picatinny Arsenal, NJ

Shear-induced particle migration is an important issue to be addressed during the processing of concentrated suspensions, which constitute various energetic formulations consisting of polymeric binders with a relatively high concentration of rigid energetic particles. Upon shear-induced particle migration during manufacturing, concentration gradients of the rigid particles are developed that lead to burn rate gradients to alter the overall burn rate behavior

---

*Presently with Procter and Gamble Inc., Cincinnati, Ohio

Address correspondence to David Fair, US Army TACOM-ARDEC, AMSRD-AAR-AEE-W, Bldg 3150, Picatinny Arsenal, NJ 07806.

of the energetic grains. Here it is demonstrated that changes in the burn rates would occur both in drag and pressure-driven processing flows under conditions in which the particle radius over the gap of the processing geometry is appreciable. Typical results are provided.

Keywords: gradient, migration, particles, processing, shear-induced

Introduction

Energetic materials like solid rocket fuels and gun propellants are suspensions consisting of a polymeric binder incorporated with rigid particles. The particles are generally symmetric with low aspect ratios and broad particle size distributions to allow achievement of relatively high solid packing ratios. The concentration of the rigid particles needs to be relatively high and in most cases approaches the maximum packing fraction of the solids (the characteristic concentration of the solid particles above which there is no fluidity). In the flow and processing of such highly filled suspensions, a number of mechanisms act to generate gradients in the concentrations of particles. For example, during pressure-driven Poiseuille flow (flow through circular tube dies or rectangular slit dies) the binder can migrate in the axial direction; i.e., flow direction [1,2]. This behavior is observed especially with concentrated suspensions filled close to their maximum packing fractions and manifests itself as the filtration of the binder as a result of the imposed pressure gradient, superimposed on the bulk flow of the suspension [2].

The second type is the migration of the non-colloidal solid particles in inhomogeneous flows of the suspension in the transverse to flow direction; i.e., in the direction of the imposed deformation rate. When the Reynolds number is greater than 10^{-3} the inertial effects give rise to the radial migration of solid particles [3,4]. However, the migration of the particles, and the resulting development of particle concentration gradients in transverse to flow direction, occur upon inhomogeneous flows even in the absence of inertial effects. Such particle migrations occur even during the creeping flows in which the prevailing

Reynolds number approaches zero. Since the shear viscosity of most energetic suspensions is very high, the flow of energetic suspensions could be considered as creeping flow and is thus subject to the migration of particles even in the absence of inertial effects.

The experimental evidence to the occurrence of the particle migrations in conditions where gradients of deformation rates exist, under conditions in which inertial effects are negligible, was first provided by Gadala-Maria and Acrivos [5], where the shear viscosity of concentrated suspensions was observed to decrease with time in Couette flow. Leighton and Acrivos [6] later showed that the observed decrease in viscosity was associated with the migration of solid particles from the high shear rate region located in between the two concentric cylinders to the low shear rate region located at the reservoir bottom of the Couette geometry. The migration of particles from high shear rate to low shear rate was further documented in wide-gap Couette flow (where shear rate is not uniform) by Abbott et al. [7] using magnetic resonance imaging. In pressure-driven channel flow (rectangular slit and capillary), a number of investigators observed the blunting of the velocity profile [8,9].

Phenomenological models of migration of neutrally buoyant, unimodal, and spherical particles suspended in Newtonian fluids across planes of shear during nonhomogeneous shear flows generally attribute the migration to irreversible interactions. By using scaling arguments, Leighton and Acrivos [6] were able to derive a general expression for the diffusive flux of particles in simple shear flow. Phillips et al. [11] used Leighton and Acrivos's [6] flux expressions to develop a diffusion equation that describes the evolution of particle concentration distributions over time. This diffusion equation assumes that there are two primary causes for particle migration; i.e., particle interactions and local variations of the concentration-dependent suspension viscosity. Phillips et al.'s [11] model was further modified by Allende and Kalyon [10] by using two different boundary conditions; i.e., the continuity of the flux at the axis of symmetry and the incorporation of apparent slip at the wall (wall slip is prevalent in the flow of concentrated suspensions including energetic suspensions). Allende and Kalyon [10] provided an extensive set of numerical analysis results in nomograph-type format to allow the ready assessment of the particle migration effects in Pouiseuille flow, elucidated the role played by wall slip, and suggested a new experimental method for quick assessment of the relative importance of particle migration effects.

Determination of Concentration and Burn Rate Gradients

There are several ways in which the irreversible interactions can lead to particle migrations in the presence of concentration and shear stress gradients. Following Phillips et al. [11], consider a suspension undergoing nonhomogeneous shear flow with a Newtonian binder. An interaction occurs when two particles embedded in adjacent shearing surfaces move past one another. Since these interactions may cause a particle to be irreversibly moved from its original streamline, a particle that experiences a higher interaction frequency from one direction than from the opposing direction will migrate normal to shearing surface and in the direction of the lower interactions frequency. This diffusion equation follows Leighton and Acrivos [6] and assumes that there are two primary causes for particle migration; i.e., gradients in collision frequency and gradients in suspension viscosity.

Consider a suspension of hard spheres with radius a in a Newtonian fluid with viscosity η_o. Assume that the particles diffuse in the Newtonian liquid at shear rate, $\dot{\gamma}$, with diffusivity D and that the Peclet number, $\mathrm{Pe} = a^2\dot{\gamma}/D$, is relatively large so that Brownian motion can be neglected. The particle flux $\vec{\mathrm{N}}_c$, occurring due to a gradient in collision frequency, is given by Phillips et al. [11]:

$$\vec{N}_c = -K_c a^2 \phi(\phi \vec{\nabla}\dot{\gamma} + \dot{\gamma}\vec{\nabla}\phi) \tag{1}$$

where K_c is a proportionality constant that needs to be determined from experimental data. The first term in Eq. (1) implies that even in the absence of a gradient in particle concentration the migration of particles will result based on the nonhomogeneous shear flow such as Poiseuille and wide-gap Couette flows. The second term in Eq. (1) states that a gradient in particle concentration will cause a spatial variation in the frequency of collisions. If a nonhomogeneous shear flow is started in a suspension with a uniform concentration distribution, ϕ_0, the first term in Eq. (1) gives rises to a flux, which in turn generates a concentration gradient and hence induces a second flux proportional to $\vec{\nabla}\phi$. Thus, the two terms in Eq. (1) are in general in opposite directions. Particles migrate from regions of high to low shear rate and from regions of high to low concentration.

In addition to the flux caused by gradients in collision frequency, it is possible that an interaction between two particles will be affected by a gradient in suspension viscosity caused by the presence of gradients in the particle concentration. The magnitude of this displacement during each irreversible interaction is scaled with the relative change in suspension viscosity; i.e., $(a/\eta_s)\vec{\nabla}\eta_s$ [11]. If each interaction causes a displacement over a characteristic distance of $O(a)$ and the interaction frequency scales as $\dot{\gamma}\phi$, then the flux $\vec{\mathrm{N}}_\eta$ due to a viscosity gradient is given by Phillips et al. [11]:

$$\vec{N}_\eta = -K_\eta a^2 \frac{\dot{\gamma}\phi^2}{\eta_s} \vec{\nabla}\eta_s \tag{2}$$

where K_η is a diffusion constant that needs to be determined from experimental data, and $\eta_s = \eta_s(\phi)$ is the shear viscosity of the concentrated suspension. Phillips et al. [11] provide a conservation equation for solid particles, which can be written in a Lagrangian reference frame as:

$$\frac{\partial\phi}{\partial t} + \vec{v} \bullet \vec{\nabla}\phi = -\vec{\nabla} \bullet (\vec{N}_c + \vec{N}_\eta) \tag{3}$$

Equation (3) is the shear-induced particle migration model developed by Phillips et al. [11] for a concentrated suspension of unimodal spheres undergoing nonhomogeneous shear flows.

This model and its modifications by Allende and Kalyon [10] form the basis for the calculations reported here to suggest that under certain conditions distributions of particle concentrations will be generated. Earlier experimental work on burn rate determination has shown that changes in the concentrations of the energetic particles will lead to changes in burn rates. For example, the experimental work of Homan et al. [12,13] using energetic thermoplastic binders, BAMO/NMMO, incorporated with RDX-type nitramine particles has clearly shown that the burn rate of the energetic suspension would be a function of the concentration of particles (Figure 5 of Homan et al. [12]). The results clearly indicate that when the concentration of the RDX particles increases, the burn rate also increases across the entire range of particle sizes considered in the 2–32 μm size range. Homan et al. [12,13] developed a response surface model for predicting burn rate equation as a function of RDX particle size and the solid loading level.

$$\begin{Bmatrix} \log a \\ n \end{Bmatrix} = \vec{\beta}_o + \vec{\beta}_1 x_1 + \vec{\beta}_2 x_2 + \vec{\beta}_{12} x_1 x_2 + \vec{\beta}_{11} x_1^2 + \vec{\beta}_{22} x_2^2 + \vec{\beta}_{112} x_1^2 x_2 + \vec{\beta}_{122} x_1 x_2^2 + \vec{\beta}_{1122} x_1^2 x_2^2 \tag{4}$$

where $x_1 = \frac{SL-60}{5}$, $x_2 = \frac{PZ-17}{15}$, $\vec{\beta}_i = 2-D$ coefficient vector, SL = solid loading level, PZ = particle size.

Assuming that the burn rate equation is in the form of Vielle's burning law:

$$BR = aP^n \tag{5}$$

or

$$\log(BR) = \log a + n^* \log P \tag{6}$$

Thus, the conditions that will generate particle concentration distributions will also lead to distributions of the burn rates. It is this premise that is investigated in this article.

Processing Flow Simplified: Flow Occurring in between Two Cylinders with a Wide Gap in between and with One of the Cylinders Rotating and the Other Stationary

Consider a concentrated energetic suspension of RDX particles undergoing nonhomogeneous shear flow in a wide-gap Couette

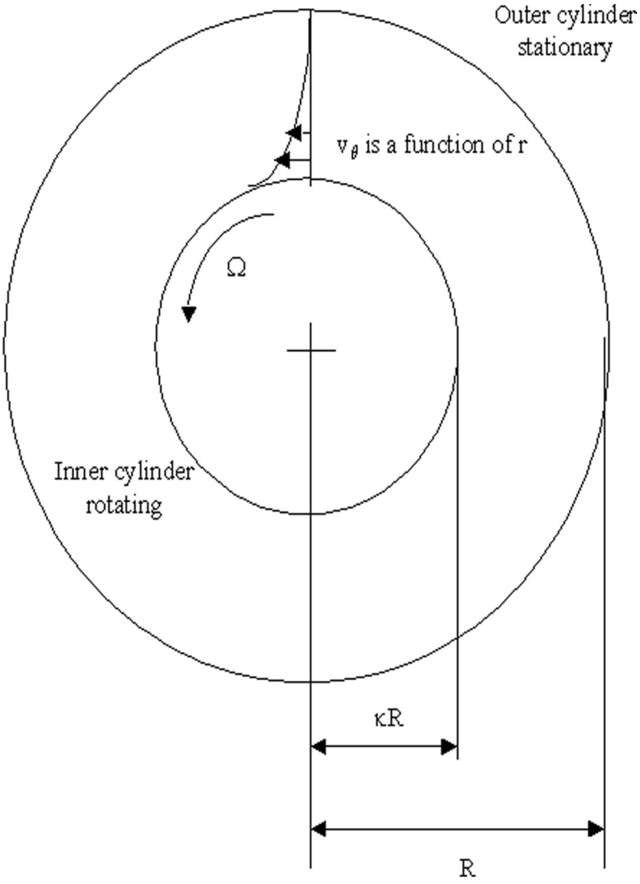

Figure 1. Wide-gap Couette geometry.

flow geometry akin to the processing of the suspension in a single-screw extruder with the pressure flow neglected (Fig. 1). In this graph the nondimensional inner cylinder radius, κ, was taken to be 0.2689. The inner cylinder with radius, κR, rotates with angular velocity, $\mathbf{\Omega}$, and outer cylinder with radius, R, is stationary, as shown in Fig. 1. The θ-component of the equation of motion in cylindrical coordinates yields

$$\frac{1}{r^2}\frac{\partial}{\partial r}(r^2\tau_{r\theta}) = 0 \tag{7}$$

The analysis for a transient Couette flow requires the solution of Eq. (8) for the case $\phi = \phi(r, t)$, where r is the radial coordinate and t is time. The diffusion equation becomes [11]:

$$\frac{\partial \phi}{\partial t} = \frac{\mathrm{a}^2}{r}\frac{\partial}{\partial r}\left\{ r\left[K_c\left(\phi^2\frac{\partial \dot{\gamma}}{\partial r} + \dot{\gamma}\phi\frac{\partial \phi}{\partial r}\right) + K_\eta\frac{\dot{\gamma}\phi^2}{\eta_s}\frac{\partial \eta_s}{\partial r}\right]\right\} \qquad (8)$$

The θ-component of the equation of motion (Eq. (7)) is solved to give an expression for the local shear rate, $\dot{\gamma}$, as a function of the concentration-dependent suspension viscosity, $\eta_s(\phi)$, which can be rendered a function of the volume fraction of the solids, ϕ, over the maximum packing fraction. The Krieger [14] model, for example, can be used to express the suspension viscosity, $\eta_s(\phi)$, as a function of the concentration, ϕ. Then, Eq. (8) is solved to give the concentration distribution $\phi = \phi(r, t)$.

The objective of such calculations is to determine the conditions of geometry, operating conditions and the characteristics of the suspension necessary for the generation of the desired concentration distribution, and hence burn rate distribution, from one surface of the propellant to the other in the transverse direction.

The steady-state distributions of the concentration are reported in Fig. 2 for $K_c/K_\eta = 0.66$. These results suggest that if a concentrated suspension of energetic particles and/or binder is placed into the gap between two cylinders, one of which is rotating and the other stationary, concentration gradients will be established with a high concentration of particles at the outer wall and a relatively low concentration of particles at the inner wall. The durations to reach these steady-state concentration distributions will be functions of the particle radius over the gap ratio. The development of the concentration distributions as a function of the number of total rotations of the inner cylinder is shown in Fig. 3 for a particle radius over the gap ratio of 0.0194 for a concentrated suspension with a volume fraction loading level of 55% of particles by volume. The nondimensional inner cylinder radius is $\kappa = 0.2689$. Comparisons with the experimental data of Phillips et al. [11] for the 800 revolutions of the inner cylinder are also included.

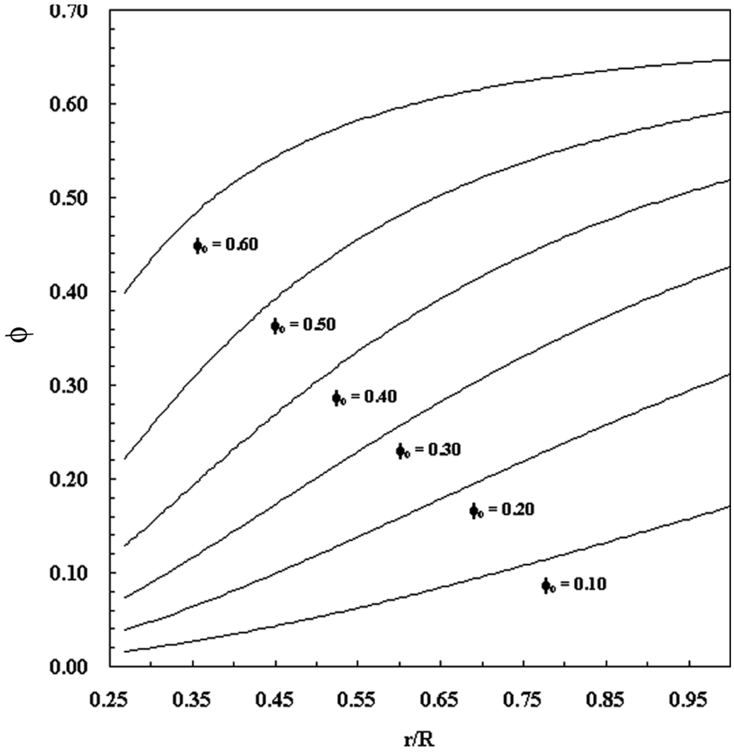

Figure 2. Steady-state concentration distribution for wide-gap Couette flow.

Thus, this concentration profile would be achieved under conditions that involve a processing geometry that follows a particle radius over the gap ratio of 0.0194. For a mean particle radius of 160 µm the gap would be 8.4 mm. If the inner cylinder is rotated 800 times under conditions that the propellant would not deteriorate and for which the temperature rise would not be significant the appreciable concentration distributions given in Fig. 3 would be obtained.

Let us consider the burn rate distributions that will evolve upon the formation of particle concentration distributions in the transverse to flow direction (Fig. 4). The typical burn rate

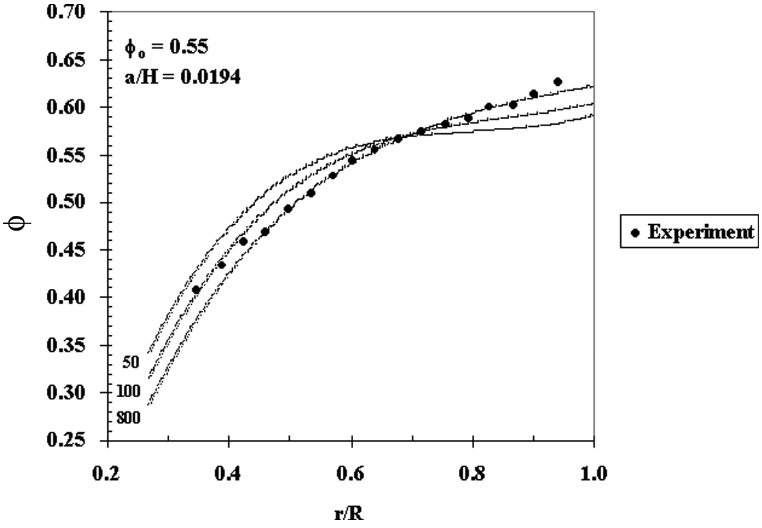

Figure 3. Transient concentration distributions as a function of inner cylinder revolutions. The experimental results are of Phillips et al. [11].

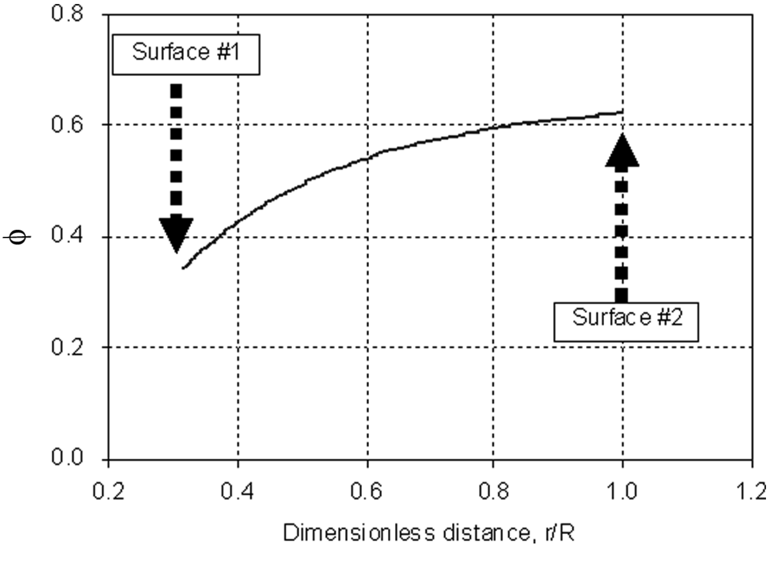

Figure 4. Concentration distribution upon shear-induced particle migration.

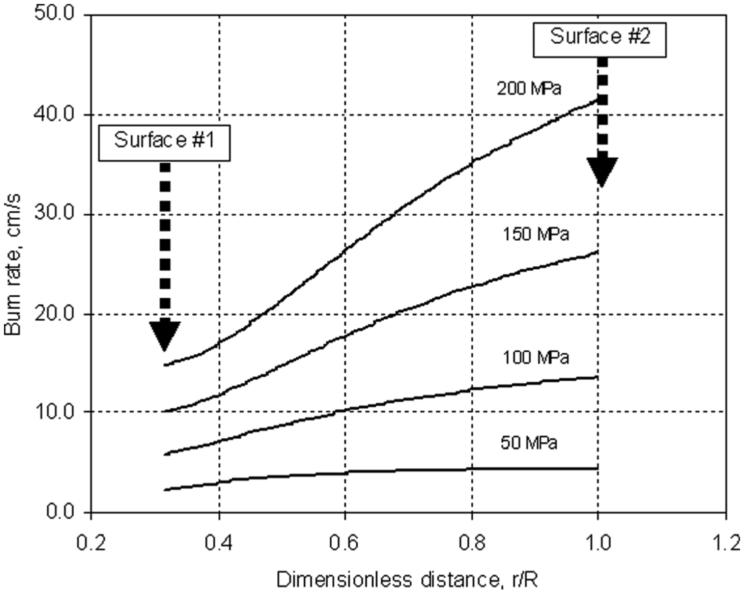

Figure 5. Burn rate versus radial location in the propellant containing RDX and BAMO/AMMO to be recovered from the annular gap between two cylinders upon Couette flow as a function of pressure.

distribution is shown in Fig. 5 for the concentration distribution of Fig. 4 as a function of pressure. Thus, for example, a slab of propellant with a slab thickness of 8.4 mm (to be recovered upon solidification from the annular space in Couette flow in between the two cylinders of Fig. 4, one of which is rotated 800 times) achieves a high rate of burn at its outer surface versus a low rate of burn at the inner surface. Burn rates in excess of 1:3 can be achieved at constant pressure. Even more significant burn rate ratios would be predicted if the pressure rise during burning of the propellant is taken into account. As the propellant burns from inside-out, the pressure will increase, and since the zones with the higher particle concentrations, located at the outer surface, will burn later than the zones with lower particle concentrations located around the inside surface, the difference in the burn rates will be even higher. This is because, as Fig. 5 indicates, the burn rate increases with increasing pressure.

Particle Migration Based Burn Rate Gradients upon Pressure-Driven Flows through Dies

The energetic formulations are frequently processed and shaped upon being forced through an extrusion die, which imparts its shape to the extruded grain. Both ram extrusion and twin-screw extrusion processes utilize dies to allow the shaping of the energetic formulations. Here simplified geometries involving a cylindrical tube or a rectangular slit are considered; however, the findings also apply to more complicated shapes. The typical die geometry and the schematics of the die flow are shown in Fig. 6.

The equation of conservation of momentum for one-dimensional flow is:

$$-\frac{1}{r^s}\frac{d}{dr}(r^s\tau_{rz}) = \frac{dP}{dz} \tag{9}$$

where r is the transverse direction, z is the axial direction, P is the pressure, τ_{rz} is the shearing stress, and exponent s is zero for rectangular slit die and one for a cylindrical tube. For simplicity, we will use here the solutions for Poiseuille flow (flow through a circular die) with the caveat that the results are also equally valid for one-dimensional rectangular slit flow and other

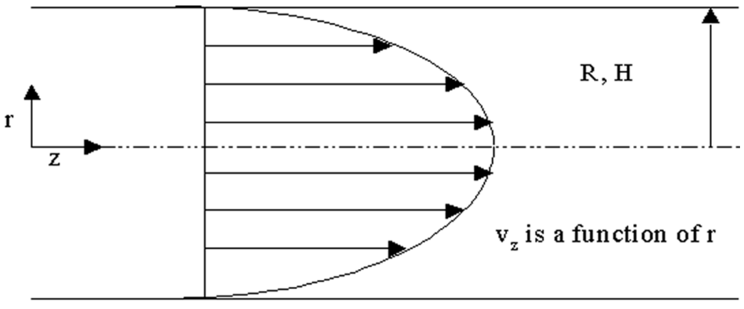

Figure 6. Flow through a rectangular slit of gap H or a circular tube with radius R.

simple shear flows. The conservation of mass requires [11]:

$$V_z \frac{\partial\phi}{\partial z} = \frac{a^2}{r}\frac{\partial}{\partial r}\left\{ r\left[K_c\left(\phi^2 \frac{\partial\dot{\gamma}}{\partial r} + \dot{\gamma}\phi\frac{\partial\phi}{\partial r}\right) + K_\eta \frac{\dot{\gamma}\phi^2}{\eta_s}\frac{\partial\eta_s}{\partial r}\right]\right\} \tag{10}$$

Equation (10) is solved with the boundary conditions of the total flux being zero at the solid surface,

$$K_c\left(\phi^2 \frac{\partial\dot{\gamma}}{\partial r} + \dot{\gamma}\phi\frac{\partial\phi}{\partial r}\right) + K_\eta \frac{\dot{\gamma}\phi^2}{\eta_s}\frac{\partial\eta_s}{\partial r} = 0 \tag{11}$$

and the symmetry condition at the axis of symmetry,

$$\frac{\partial\phi}{\partial r} = 0 \tag{12}$$

During the flow of suspensions, a binder-rich apparent slip layer develops with thickness δ. If this thickness is stable, the relationship between the wall shear stress and slip velocity (Navier's slip condition) is given by the following expression for a Newtonian binder (for $\delta \ll R$):

$$U_s = \frac{\delta}{\eta_o}\tau_w = \beta\tau_w = V_z(R-\delta, z) \tag{13}$$

where η_o is the shear viscosity of the Newtonian binder and R is the radius of the capillary. Various techniques are available to determine the Navier's slip coefficient, β, using viscometric flows [15–17].

The particle concentration, ϕ, is assumed to be uniform initially [18]:

$$\phi = \phi_o \quad \text{for } 0 \le r \le R \quad \text{at } z = 0 \tag{14}$$

The coupled Eqs. (9) and (10) are solved in conjunction with the Krieger [14] model of the concentration-dependent suspension viscosity using a numerical method [19]. For example, the steady-state distributions of the concentration profiles are given in Fig. 7 for various values of the initial concentration of the solid particles ϕ_0, in the range of 10–60% by volume. The fully developed profiles suggest that there would be significant depletion of the particle concentration at the wall of the die

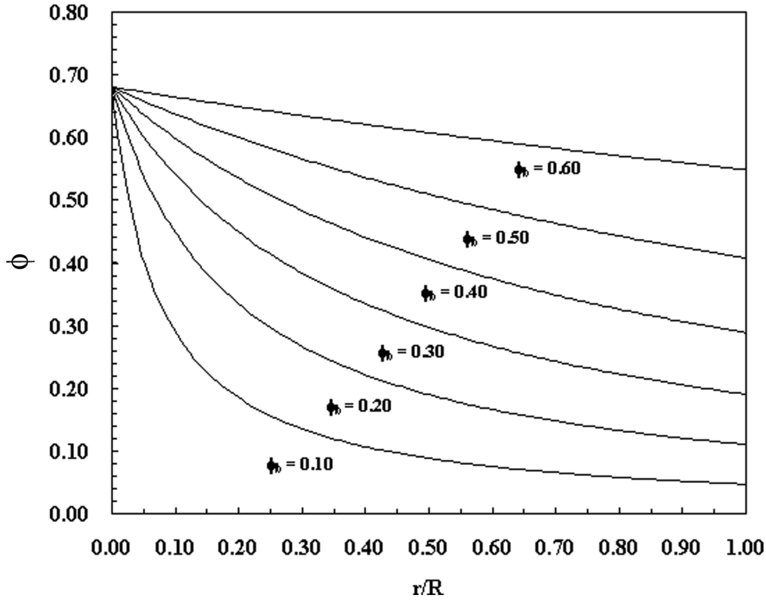

Figure 7. Fully-developed concentration distribution for steady-state Poiseuille flow.

and significant increase of the concentration of the particles as one approaches the axis of the symmetry. Thus, under such fully developed conditions one would obtain a significant variation of the particle concentration between the wall and the center.

The developments of the concentration distribution in the cylindrical die as a function of the length over the diameter, D, ratio of the die, i.e., L/D are shown in Fig. 8. The initial concentration of the particles is 45% by volume. The ratio of the particle radius to the radius of the tubular die is 0.0256. As the L/D ratio increases, the variation of the concentrations across the gap becomes more pronounced. Comparisons with the experimental data of Hampton et al. [18] are also included.

For example, for a channel length over diameter ratio of 100, the volume fraction of particles becomes 0.37 at the wall and 0.68 at the axis of symmetry. If the radius of the tubular die is taken as 10 mm, then the total length of the die necessary

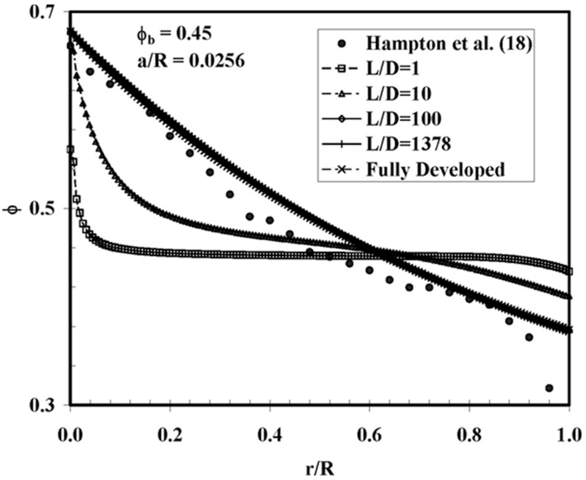

Figure 8. Particle concentration distributions for a suspension with 45% by volume solids at various capillary die length over diameter ratios and comparison with the experimental results of Hampton et al. [18].

to give rise to this concentration distribution would become 1 m. The diameter of the particles is 0.25 mm (unimodal). Again for the same material, i.e., the RDX/ETPE formulation, the burn rate profile of the propellant of this example is given in Fig. 9. These results suggest that the burn rate at the surface of the cylindrical energetic grain would have a burn rate that would be about three times smaller than the burn rate of the propellant at the axis of the symmetry of the propellant grain. This is again a significant variation and such variations would be affected significantly by the selection of the geometry for processing and the material (especially the particle size distributions).

On the other hand, the conditions that increase the channel gap over the particle diameter ratio would reduce the particle migration effect during the processing of energetics. The decrease of the length over the gap of the die would also decrease the shear induced particle migration effect and the differences in burn rate variation across the extruded grain.

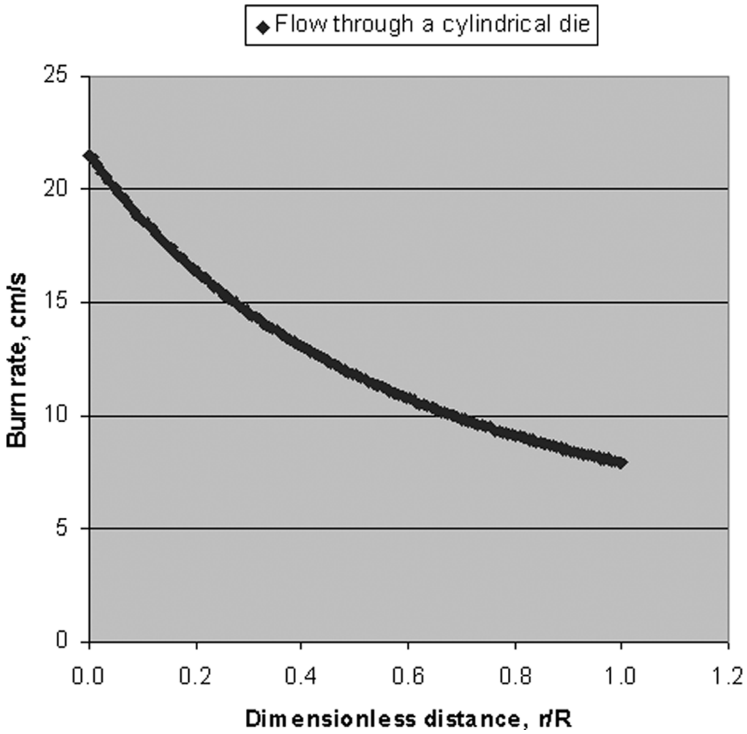

Figure 9. Burn rate versus location in a cylindrical grain of propellant exposed to flow in die with a length over the diameter ratio of 100. The particle radius over the die radius is 0.0256. The mean particle diameter is 0.25 mm.

Allende and Kalyon [10] have provided easy-to-use nomographs and simple experimental means to allow the apriori determination of conditions under which shear induced particle migration effects become significant, provided that the wall slip behavior of the suspension is characterized [20]. It should be noted that the use of expanding and converging geometries during processing have the additional potential of inducing significant alterations in the distributions of concentrations of particles [21] and such changes in geometries should be considered.

Early calculations related to the extrusion of a grain with circular cross section indicate only modest increases in performance due to surface area loss during burning. However, geometries with a rectangular cross section should greatly reduce the loss of surface area with time and are expected to show substantial improvements in ballistic performance. These shapes may be formed by either laminating the product of the Couette flow device or directly extruding a rectangular cross section or ribbon.

The results reported in this paper provide proof of principle that a significant shear induced concentration gradient could be established upon the processing of energetic formulations for particles that are sufficiently large. Further work to explore and exploit this technology is strongly recommended.

Conclusions

Burn rate differentials can be inadvertently generated during the processing of energetic suspensions due to differences in the deformation rate that the energetic material is exposed to. Particles migrate away from high shear rate regions, giving rise to particle-depleted regions at the high shear rate locations [5–7]. On the other hand, low shear rate regions in the flow achieve greater particle concentrations. The generated differences in particle concentrations give rise to differences in burn rate with the burn rate increasing at locations with increased particle concentration. The safety aspect of differential burn rate generation should also be considered. On the other hand, such differences in burn rate can also be generated by design and can allow the fabrication of functionally graded propellant strands with desired burn rate gradients.

Acknowledgments

This project is supported by U.S. Army ARDEC, contract W15QKN-05-D-0011, for which we are grateful.

References

[1] Yilmazer, U., C. Gogos, and D. M. Kalyon. 1989. Mat formation and unstable flows of highly filled suspensions in capillaries and continuous processors. *Polymer Composites*, 10(4): 242–248.

[2] Yaras, P., D. M. Kalyon, and U. Yilmazer. 1994. Flow instabilities in capillary flow of concentrated suspensions. *Rheologica Acta*, 33: 48–59.

[3] Segré, G. and A. Silberberg. 1961. Radial particle displacements in Poiseuille flow of suspensions. *Nature*, 189: 209–210.

[4] Goldsmith, H. L. and S. G. Mason. 1961. Axial migration of particles in Poiseuille flow. *Nature*, 190: 1095–1096.

[5] Gadala-Maria, F. and A. Acrivos. 1980. Shear-induced structure in a concentrated suspension of solid spheres. *Journal of Rheology*, 24: 799–814.

[6] Leighton, D. and A. Acrivos. 1987. The shear-induced migration of particles in concentrated suspensions. *Journal of Fluid Mechanics*, 181: 415–439.

[7] Abbott, J. R., N. Tetlow, A. L. Graham, S. A. Altobelli, E. Fukushima, L. A. Mondy, and T. S. Stephens. 1991. Experimental observations of particle migration in concentrated suspensions: Couette flow. *Journal of Rheology*, 35: 773–795.

[8] Karnis, A., H. L. Goldsmith, and S. G. Mason. 1966. The kinetics of flowing dispersions. I. Concentrated suspensions of rigid particles. *Journal of Colloid and Interface Science*, 22: 531–553.

[9] Koh, C. J., P. Hookham, and L. G. Leal. 1994. An experimental investigation of concentrated suspension flows in a rectangular channel. *Journal of Fluid Mechanics*, 266: 1–32.

[10] Allende, M. and D. Kalyon. 2000. Assessment of particle-migration effects in pressure-driven viscometric flows. *Journal of Rheology*, 44(1): 79–90.

[11] Phillips, R. J., R. C. Armstrong, R. A. Brown, A. L. Graham, and J. R. Abbott. 1992. A constitutive equation for concentrated suspensions that accounts for shear-induced particle migration. *Physics of Fluids A*, 4: 30–40.

[12] Homan, B., D. Devynck, P. Kaste, R. Lieb, D. Bullock, and A. Juhasz. 2001. *BNMO/NMMO/RDX TPE Propellant Performance as a Function of Nitramine Particle Size and Solids Loading*. U.S. Army Research Laboratory Report, ARL-TR-2624 Aberdeen, MD.

[13] Homan, B., D. Webb, and P. Kaste. 2002. *Statistical Evaluation of the Effects of Particles Size and Solids Loading on the Burning Rate of an RDX-Energetic Thermoplastic Elastomer Propellant Matrix*. U.S. Army Research Laboratory Report, ARL-TR-2854, Aberdeen, MD.

[14] Krieger, I. M. 1972. Rheology of monodisperse lattices. *Advances in Colloid and Interface Science*, 3: 111–136.

[15] Kalyon, D. 2005. Apparent slip and viscoplasticity of concentrated suspensions. *Journal of Rheology*, 49(3): 621–640.

[16] Kalyon, D. M., P. Yaras, B. Aral, and U. Yilmazer. 1993. Rheological behavior of a concentrated suspension: a solid rocket fuel simulant. *Journal of Rheology*, 37: 35–53.

[17] Aral, B. K. and D. M. Kalyon. 1994. Effects of temperature and surface roughness on time-dependent development of wall slip in steady torsional flow of concentrated suspensions. *Journal of Rheology*, 38: 957–972.

[18] Hampton, R., A. Mammoli, A. Graham, N. Tetlow, and S. Altobelli. 1997. Migration of particles undergoing pressure driven flow in a circular conduit. *Journal of Rheology*, 41: 621–640.

[19] Allende, M. 2000. *Shear Induced Particle Migration in Suspensions of Non-Colloidal Particles*. PhD Thesis, Stevens Institute of Technology, Hoboken, NJ.

[20] Yilmazer, U. and D. M. Kalyon. 1989. Slip effects in capillary and parallel disk torsional flows of highly filled suspensions. *Journal of Rheology*, 33: 1197–1212.

[21] Moraczewski, T., H. Tang, and N. C. Shapley. 2005. Flow of a concentrated suspension through an abrupt, axisymmetric expansion measured by nuclear magnetic resonance imaging. *Journal of Rheology*, 49(6): 1409–1428.